LIDAR-DERIVED ELEVATION DATA FOR TUNTUTULIAK, SOUTHWEST ALASKA, COLLECTED AUGUST 18, 2021

Jenna M. Zechmann, Andrew M. Herbst, and Richard M. Buzard

Raw Data File 2023-17

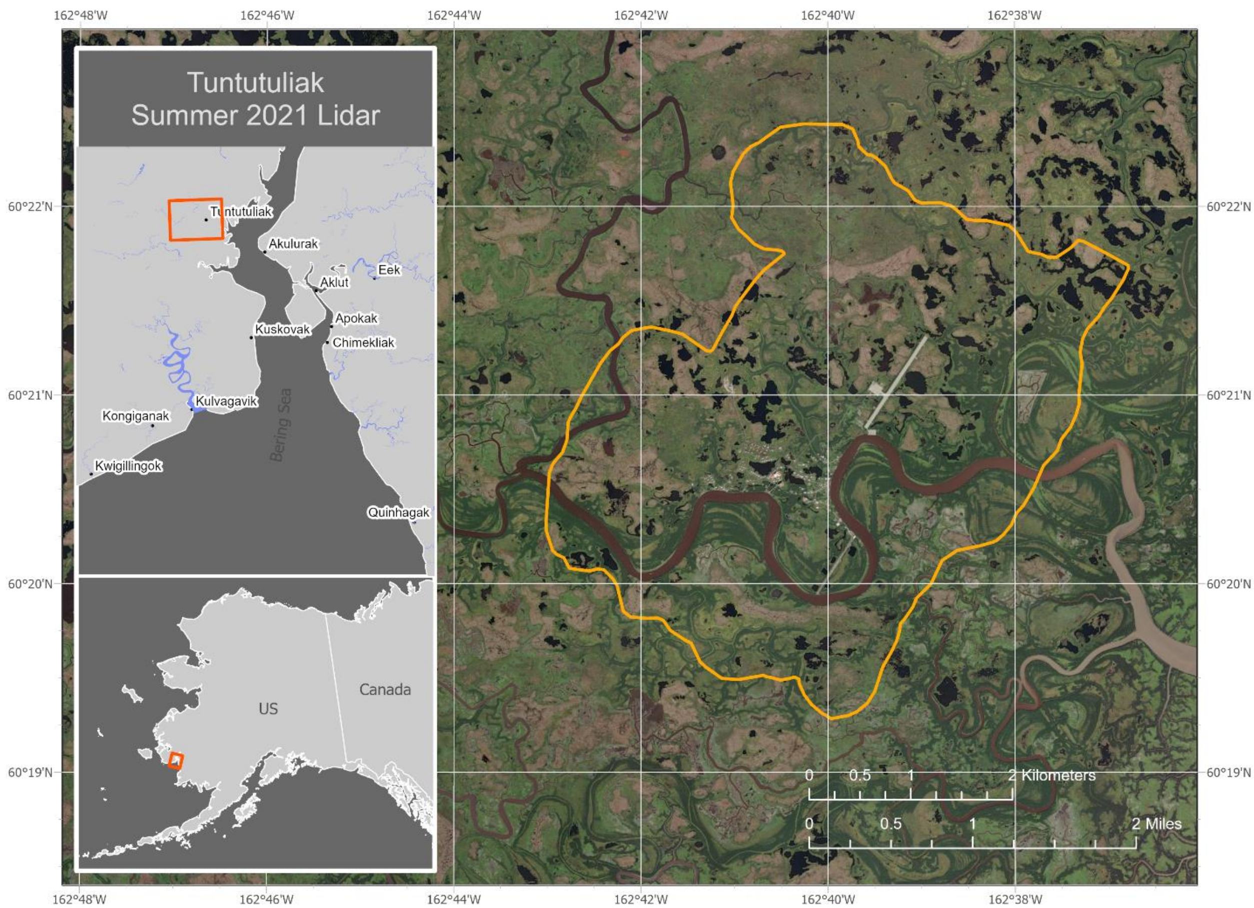

Location map of survey area with orthometric image.

This report has not been reviewed for technical content or for conformity to the editorial standards of DGGS.

2023
STATE OF ALASKA
DEPARTMENT OF NATURAL RESOURCES
DIVISION OF GEOLOGICAL & GEOPHYSICAL SURVEYS

STATE OF ALASKA
Mike Dunleavy, Governor

DEPARTMENT OF NATURAL RESOURCES
John Boyle, Commissioner

DIVISION OF GEOLOGICAL & GEOPHYSICAL SURVEYS
Melanie Werdon, State Geologist & Director

Publications produced by the Division of Geological & Geophysical Surveys are available to download from the DGGS website (dggs.alaska.gov). Publications on hard-copy or digital media can be examined or purchased in the Fairbanks office:

Alaska Division of Geological & Geophysical Surveys (DGGS)
3354 College Road | Fairbanks, Alaska 99709-3707
Phone: 907.451.5010 | Fax 907.451.5050
dggspubs@alaska.gov | dggs.alaska.gov

DGGS publications are also available at:

Alaska State Library, Historical
Collections & Talking Book Center
395 Whittier Street
Juneau, Alaska 99801

Alaska Resource Library and
Information Services (ARLIS)
3150 C Street, Suite 100
Anchorage, Alaska 99503

Suggested citation:
Zechmann, J.M., Herbst, A.M., and Buzard, R.M., 2023, Lidar-derived elevation data for Tuntutuliak, Southwest Alaska, collected August 18, 2021: Alaska Division of Geological & Geophysical Surveys Raw Data File 2023-17. https://doi.org/10.14509/31033

LIDAR-DERIVED ELEVATION DATA FOR TUNTUTULIAK, SOUTHWEST ALASKA, COLLECTED AUGUST 18, 2021

Jenna M. Zechmann[1], Andrew M. Herbst[1], and Richard M. Buzard[2]

INTRODUCTION

The Alaska Division of Geological & Geophysical Surveys (DGGS) used aerial lidar to produce a classified point cloud, digital surface model (DSM), digital terrain model (DTM), and intensity model of Tuntutuliak, Southwest Alaska (cover figure) during leaf-on ground conditions. The survey provides snow-free surface elevation data for assessing coastal erosion and flooding hazards. Ground control data and aerial lidar data were collected on August 18, 2021, and subsequently processed using a suite of geospatial processing software. This data collection is released as a Raw Data File with an open end-user license. All files are available at https://doi.org/10.14509/31033.

LIST OF DELIVERABLES

Classified Points

DSM and DTM

Intensity Image

Metadata

MISSION PLAN

Aerial Lidar Survey Details

DGGS used a Riegl VUX1-LR laser scanner integrated with a global navigation satellite system (GNSS) and Northrop Grumman LN-200C inertial measurement unit (IMU). The lidar integration system was designed by Phoenix LiDAR Systems. The sensor can collect up to 820,000 points per second at a range of up to 150 m. The scanner operated with a pulse refresh rate of 400,000 pulses per second at a scan rate of 200 lines per second. We used a Cessna 180 fixed-wing platform to survey from an elevation of ~200 m above ground level, at a ground speed of ~40 m/s, and with a scan angle set from 80 to 280 degrees. The total survey area covers ~19 km^2 (cover figure).

Weather Conditions and Flight Times

We flew the aerial survey on August 18, 2021, taking off from Bethel Airport and landing at Tuntutuliak Airport (fig. 1). Data was collected from 12:10 pm to 1:10 pm AKST. The weather throughout the survey was clear, with no wind.

---

[1] Alaska Division of Geological & Geophysical Surveys, 3354 College Road, Fairbanks, AK 99709

[2] University of Alaska Fairbanks Arctic Coastal Geoscience Lab, 900 Yukon Drive, Fairbanks, AK 99775

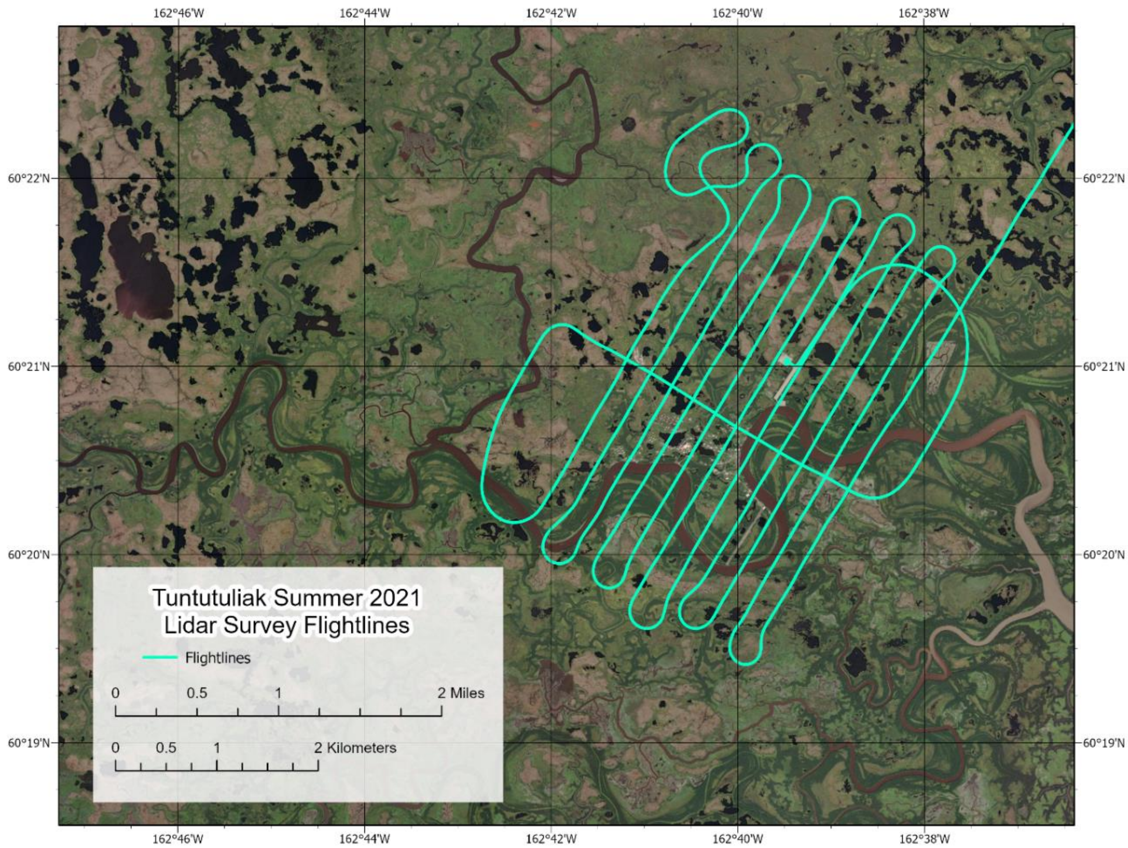

Figure 1. Lidar data collection flightlines.

PROCESSING REPORT

Lidar Dataset Processing

We processed point data in SDCimport software for initial filtering and multiple-time-around (MTA) disambiguation. MTA errors, corrected in this process, result from ambiguous interpretations of received pulse time intervals and occur more frequently with higher pulse refresh rates. We processed IMU and GNSS data in Inertial Explorer, and we used Spatial Explorer software to integrate flightline information with the point cloud. We calibrated the point data at an incrementally precise scale of sensor movement and behavior, incorporating sensor velocity, roll, pitch, and yaw fluctuations throughout the survey.

We created macros in Terrasolid software and classified points in accordance with American Society for Photogrammetry and Remote Sensing (ASPRS) 2019 guidelines. Once classified, we applied a geometric transformation and converted the points from ellipsoidal heights to GEOID12B (Alaska) orthometric heights.

We used ArcGIS Pro to derive raster products from the point cloud. The DSM was interpolated from maximum return values from the ground, vegetation, bridge deck, and building classes using a binning method. The DTM was interpolated from all ground class returns, also using a binning method and minimum values. In ArcGIS Pro, we produced an intensity image by binning and averaging ground, vegetation, building, and bridge deck classes.

Classified Point Cloud

Classified point cloud data are provided in compressed LAZ format. Data are classified following ASPRS 2019 guidelines (table 1) and contain return and intensity information. The average pulse spacing is 55.9 cm, and the average density is 3.21 pts/m^2 (fig. 2).

Table 1. Pointcloud class code definitions.

Class Code	Description
1	Unclassified
2	Ground
3	Low Vegetation (≥0.05, <0.2 meters above the ground)
4	Medium Vegetation (≥0.2, <3 meters above the ground)
5	High Vegetation (≥3, ≤40 meters above the ground)
6	Building
7	Low Noise
10	Bridge Deck
18	High Noise

Digital Surface Model

The DSM represents surface elevations, including heights of vegetation, buildings, boardwalks, powerlines, etc. The DSM is a single-band, 32-bit GeoTIFF file of 50-centimeter resolution. No Data value is set to -3.40282306074e+38 (32-bit, floating-point minimum).

Digital Terrain Model

The DTM represents bare earth elevations, excluding vegetation, bridges, buildings, etc. The DTM is a single-band, 32-bit float GeoTIFF file of 50-centimeter resolution. No Data value is set to -3.40282306074e+38.

Lidar Intensity Image

The lidar intensity image depicts the relative amplitude of reflected signals contributing to the point cloud. Lidar intensity is primarily a function of scanned object reflectance in relation to the signal frequency, is dependent on ambient conditions, and is not necessarily consistent between separate scans. The intensity image is a single-band, 32-bit float GeoTIFF file of 1-meter resolution. No Data value is set to -3.40282306074e+38.

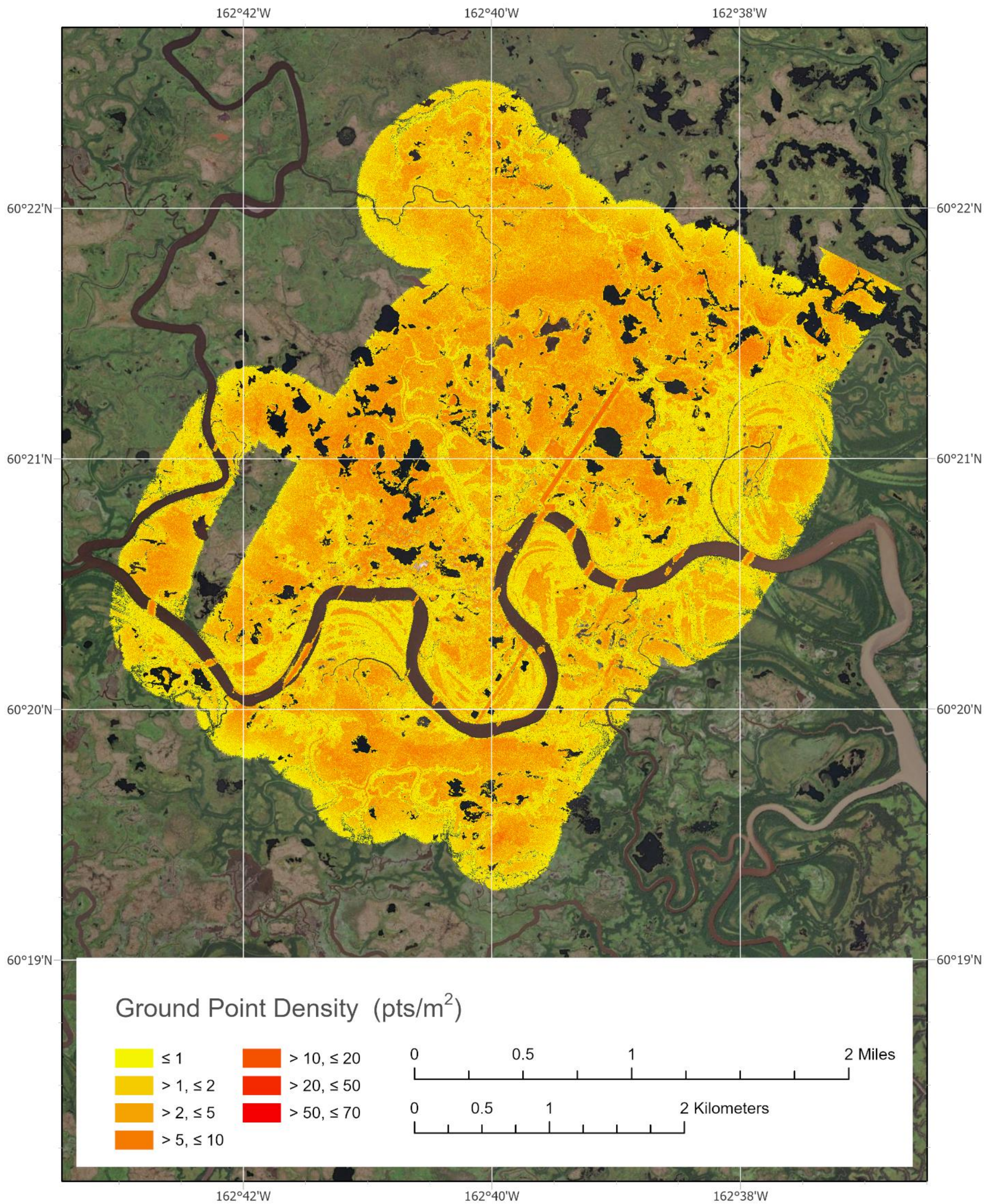

Figure 2. Ground point density for the survey displayed as a 1-meter raster.

SURVEY REPORT

Ground Survey Details

We deployed a Trimble R10 GNSS receiver at Tuntutuliak Airport. It provided a base station occupation and real-time kinematic (RTK) corrections to points we surveyed with a rover Trimble R8 GNSS receiver (internal antenna). We collected 43 ground control and checkpoints to use for calibration and to assess the vertical accuracy of the point cloud. Points were collected on bare earth, boardwalks, and vegetation (tall grass or alder).

Coordinate System and Datum

We processed and delivered all data in NAD83 (2011) UTM3N and vertical datum NAVD88 GEOID12B.

Horizontal Accuracy

We did not measure horizontal accuracy for this collection.

Vertical Accuracy

We measured a mean offset of 48.8 cm between 33 control points and the point cloud (app. 1). We reduced this offset to 0.1 cm by performing a vertical transformation of the lidar point data. We used ten checkpoints to determine the non-vegetated vertical accuracy (NVA) of the point cloud ground class using a Triangulated Irregular Network (TIN) approach. We calculated the project NVA to have a root mean square error (RMSE) of 3.7 cm (app. 2). We evaluated the relative accuracy for this dataset as the interswath overlap consistency and measured it at 6.7 cm RMSE.

Data Consistency and Completeness

This is a full-release dataset. There was no over-collect except for aircraft turns that were eliminated from the dataset. The data quality is consistent throughout the survey.

ACKNOWLEDGMENTS

This survey area is on the traditional homelands of the Yup'ik people. Data collection and processing were funded by the National Fish and Wildlife Foundation (now known as the National Coastal Resilience Fund), grant number 0318.20.069342, through the Alaska Native Tribal Health Consortium. We thank Clearwater Air for their aviation expertise and contribution to these data products. The views and conclusions contained in this document are those of the authors and should not be interpreted as necessarily representing the official policies, either expressed or implied, of the U.S. Government.

REFERENCES

The American Society for Photogrammetry & Remote Sensing, 2019, LAS Specification 1.4 - R15. https://www.asprs.org/wp-content/uploads/2019/07/LAS_1_4_r15.pdf

APPENDIX 1: GROUND CONTROL POINTS

GCP	Easting (m)	Northing (m)	Checkpoint Z (m)	Pointcloud Z (m)	Dz (m)
1	628947.688	6691416.710	3.519	4.010	0.491
2	629008.961	6691336.599	3.659	4.130	0.471
3	628764.026	6690834.618	3.250	3.840	0.590
4	628950.056	6691424.229	3.504	4.110	0.606
5	628642.665	6692005.349	2.770	3.220	0.450
6	628849.247	6692041.968	3.481	3.910	0.429
7	628794.965	6691837.109	3.191	3.660	0.469
8	629121.097	6691246.856	3.196	3.640	0.444
9	627913.547	6691978.414	3.088	3.540	0.452
10	628114.909	6692054.747	3.657	4.100	0.443
11	629157.918	6692750.350	7.678	8.110	0.432
12	628917.423	6691455.505	3.990	4.430	0.440
13	629008.966	6691336.598	3.659	4.130	0.471
14	629063.922	6691292.835	3.421	3.900	0.479
15	628891.368	6691012.056	4.162	4.650	0.488
16	628810.123	6690880.726	4.084	4.570	0.486
17	628735.884	6690750.028	4.031	4.530	0.499
18	628587.094	6691630.027	4.170	4.610	0.440
19	627980.524	6691897.689	3.549	3.980	0.431
20	628038.465	6691818.939	4.054	4.470	0.416
21	628362.790	6692043.958	3.944	4.460	0.516
22	628753.802	6692018.937	3.162	3.600	0.438
23	628821.527	6691542.266	3.336	3.790	0.454
24	629114.864	6691251.875	3.353	3.790	0.437
25	628610.451	6691699.001	3.068	3.560	0.492
26	628105.490	6691811.571	3.524	4.010	0.486
27	627856.098	6691859.890	3.739	4.190	0.451
28	627597.863	6691827.055	3.904	4.390	0.486
29	627804.115	6691894.635	3.373	3.880	0.507
30	627944.293	6692073.198	2.815	3.310	0.495
31	628803.879	6691911.514	3.390	4.060	0.670
32	627629.725	6691841.413	3.623	4.280	0.657
33	628154.238	6692133.040	3.348	3.920	0.572
Average dz (m)	0.488				
Minimum dz (m)	0.416				
Maximum dz (m)	0.670				
Average magnitude error (m)	0.488				
Root mean square error (m)	0.492				
Standard deviation	0.064				

APPENDIX 2: CHECK POINTS

Check Point	Easting (m)	Northing (m)	Checkpoint Z (m)	Corrected Pointcloud Z (m)	Dz (m)
1	627490.715	6691796.551	2.859	2.860	0.001
2	628273.670	6692098.079	4.595	4.660	0.065
3	627812.806	6691738.590	3.979	3.940	-0.039
4	628700.170	6691608.043	3.851	3.890	0.039
5	628307.419	6691771.824	3.092	3.020	-0.072
6	628984.457	6691160.389	3.713	3.720	0.007
7	629237.273	6692699.639	7.289	7.280	-0.009
8	627720.862	6691889.123	2.716	2.720	0.004
9	628798.995	6691919.066	3.568	3.560	-0.008
10	628733.497	6691749.887	3.304	3.330	0.026
Average dz (m)	0.001				
Minimum dz (m)	-0.072				
Maximum dz (m)	0.065				
Average magnitude error (m)	0.027				
Root mean square error (m)	0.037				
Standard deviation (m)	0.038				